

# Investigation on shock wave focusing in 2-stage PDE

Hao ZENG<sup>1,2</sup>, Li-ming HE<sup>2</sup>, Wei CHEN<sup>2</sup>

1.Center for Combustion energy, Tsinghua University; 2.Institute of Engineering, Air Force Engineering University

1.Beijing, China; 2.Xi'an, Shanxi, China

**Abstract:** A 2-stage pulsed detonation device was assembled and examined in an experimental program. Non-reaction experiments and initiation experiments on shock wave focus were carried out respectively. Non-reaction experiments were carried out to find better configuration of resonator, then the best resonator was chosen to carry out initiation experiments using petrol as fuel. The influences of resonator size, resonator curvature, resonator stretch angle, resonator airflow exit area, nozzle diverging angle and ' $L$ ' on shock wave focus were studied. It was found that with the increase of partial-spherical resonator size,  $\alpha$ -frequency decreases and the quantity of  $\beta$ -frequency decreases; effectiveness of the partial-spherical resonator with  $D=74\text{mm}$  is the best. As the curvature of resonator increases,  $\alpha$ -frequency increases and the dynamic pressure amplitude of resonator bottom decreases. As the incidence angle of resonator increases, resonant frequency increases. As airflow exit area decreases, resonant frequency of resonator increases and the dynamic pressure amplitude of resonator bottom increases. As nozzle diverging angle increases, the highest  $\alpha$ -frequency increases and the quantity of  $\beta$ -frequency increases. When the nozzle diverging angle is  $30^\circ$ , the dynamic pressure amplitude of resonator bottom is maximal. As ' $L$ ' increases, resonant frequency decreases and the dynamic pressure amplitude of resonator bottom decreases. During initiation experiments, three distinct combustion models were found.

**Key words:** 2-stage pulse detonation engine; detonation wave; shock wave focus; shock wave; initiation

Detonation waves are incorporated into pulsed detonation engines (PDEs), where the high exit velocity of the wave enables thrust during high-speed flight, and the pressure increase behind the detonation wave overcomes the force of the stagnation pressure in front of the engine [1,2,3]. In the last few years, a new concept has been proposed that offers a solution to these challenges: the 2-stage pulse detonation engine [4]. The 2-stage pulse detonation engine works with traditional aviation fuels, requires no mechanical valves, and achieves high operating frequencies ( $>1\text{kHz}$ ). In the first stage of a 2-stage PDE, a very rich fuel-air mixture is partially oxidized under constant pressure. The resulted products are mixed with additional air and directed into a resonator. A detonation is then initiated in this resonator via jet interaction and shock focusing. Ivett A. Leyva and Venkat Tangirala studied the non-reacting flow field in a resonant cavity. Four configurations were studied numerically and experimentally. CFD codes are anchored and validated using the measured data (frequency and amplitude of pressure oscillations, and high speed Schlieren images) from the 2-D planar configuration and then applied to the research of a 2-D axisymmetric configuration [5]. Keith R McManus and Anthony J. Dean assembled a 2-stage pulsed detonation device and examined in an experimental program [6].

The detonation initiation process is critical to the success of this concept. But, the details of the flow interaction within the resonator have not been well understood. A thorough understanding of the transient flow field in the resonator and its role in detonation initiation is necessary for successful design of a 2-stage PDE. The following sections describe

experiments that were aimed at elucidating the effectiveness of non-reaction shock wave focus in resonators of 2-stage PDE. The present study comprises a description and summary on experimental results of the influence of resonator size, resonator curvature, resonator stretch angle, resonator airflow exit area, nozzle diverging angle and the distance from resonator to toroidal incidence nozzle on shock wave focus. The experimental system includes shock initiation apparatus, air supply system, oil supply system, pre-ignition control system of pre-combustion, and the data acquisition system. Certain processes must occur in a cyclical fashion for repeating detonations to occur. If one draws an analogy between the 2-stage device and a simple tube PDE, a process cycle can be constructed as is shown in Figure 1. Schematic representation of 2-stage PDE principle experimental system is shown in Figure 2 and Figure 3. Computational and experimental efforts were used to examine different methods of facilitating detonation initiation in the 2-stage resonator. In papers [7,8,9], chemical model were found and detonation initiation in resonator were numerical simulated by authors. The experimental apparatus consists of a series of subsystems which, when coupled together, comprise a 2-stage pulsed combustion assembly. The resonator was designed to fit downstream of the pre-combustor in a modular fashion. Figure 4 shows a cross-section of the resonator assembly. In this paper, the resonator is supplied with air flow stream only. The stream enters the resonator cup through an toroidal slot located at the periphery of the cup. The flow then exits the cup. The resonator cup is open to the atmosphere.

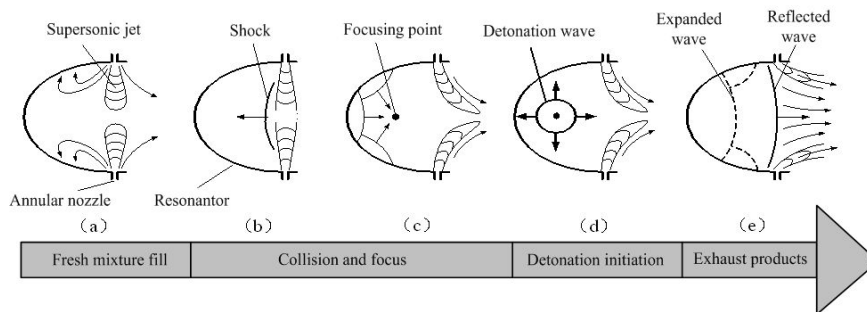


Fig.1. Schematic showing the major processes that occur within a PDE cycle

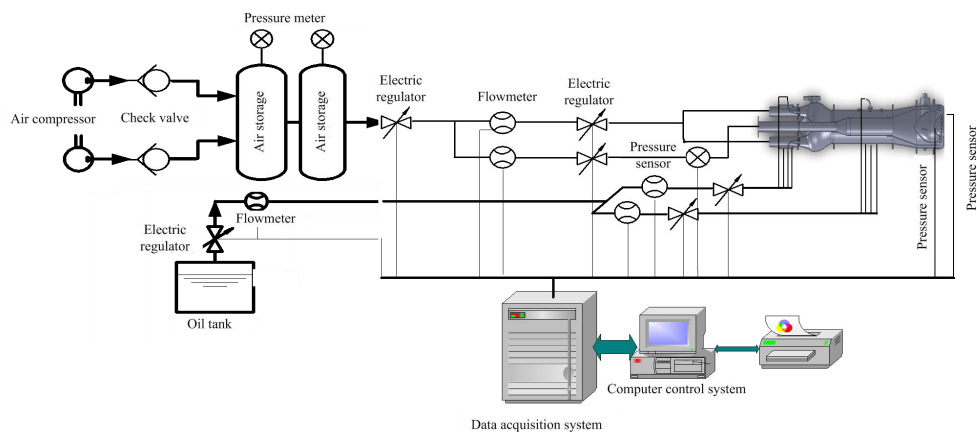


Fig.2 Schematic representation of 2-stage PDE principle experimental system



Fig.3 Picture of 2-stage PDE principle experimental system

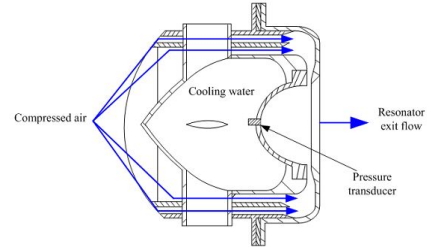


Fig.4 Cross-section of resonator assembly

From former numerical simulation results, we concluded that resonator performance can be influenced by resonator configuration. These factors including incidence angles, resonator airflow exit area, nozzle diverging angle and the distance 'L' from resonator to incidence nozzle (as showed in figure 6- figure 9). It is necessary to find which resonator configuration has better shock wave focusing performance. The research of this paper mainly contain two sections, in the first section we carry out non-reaction experiments to find better configuration of resonator; in the second section, we choose the best resonator to carry out initiation experiments using petrol as fuel.

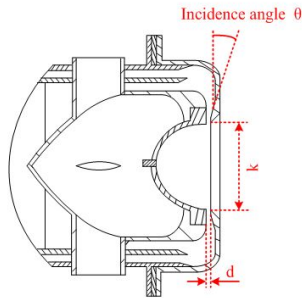


Fig.6 Incidence angle adjustment rings

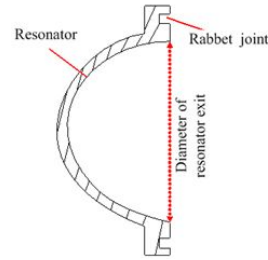


Fig.7 The flake of adjustment distance between resonator and incidence nozzle

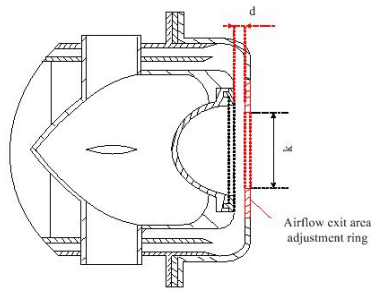


Fig.8 Airflow exit area adjustment rings

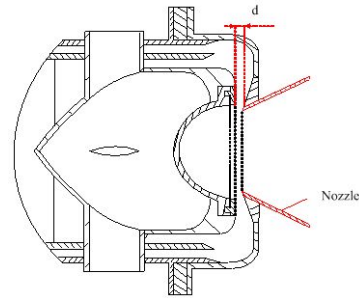


Fig.9 Nozzles with various diverging angle

## Results and Discussion

### 1.Non-reaction experiments

Figure 10 show the spectrum waterfall diagram and time domain figure of dynamic pressure of hemispherical resonator bottom ( $D=70\text{mm}$  hemisphere resonator,  $k=70\text{ mm}$ ,  $d=4.2\text{ mm}$ ). As can be seen from figure 10, for one case, the frequency ranges from 20.2 kHz to 20.36 kHz when the incidence pressure is 0.4MPa-0.7MPa; in another case, the frequency ranges from 15.84 kHz to 15.89 kHz when the incidence pressure is 0.62MPa-0.7MPa. The dynamic pressure amplitude at the resonator bottom ranges from 0.38MPa to 0.55MPa.

The experiment results show that the resonant frequency of the resonator generally has two types: one appears with the incidence pressure from 0.4MPa to 0.7MPa, recorded as 'α-frequency', is caused by toroidal jet incidence; the other appears in a certain incidence pressure range, recorded as 'β-frequency', is caused by shock wave focus in the resonator.

As can be seen from figure 10, the dynamic pressure at the hemispherical resonator bottom ranges from 0.38MPa to 0.55MPa when the incidence pressure is 0.4MPa-0.7MPa.

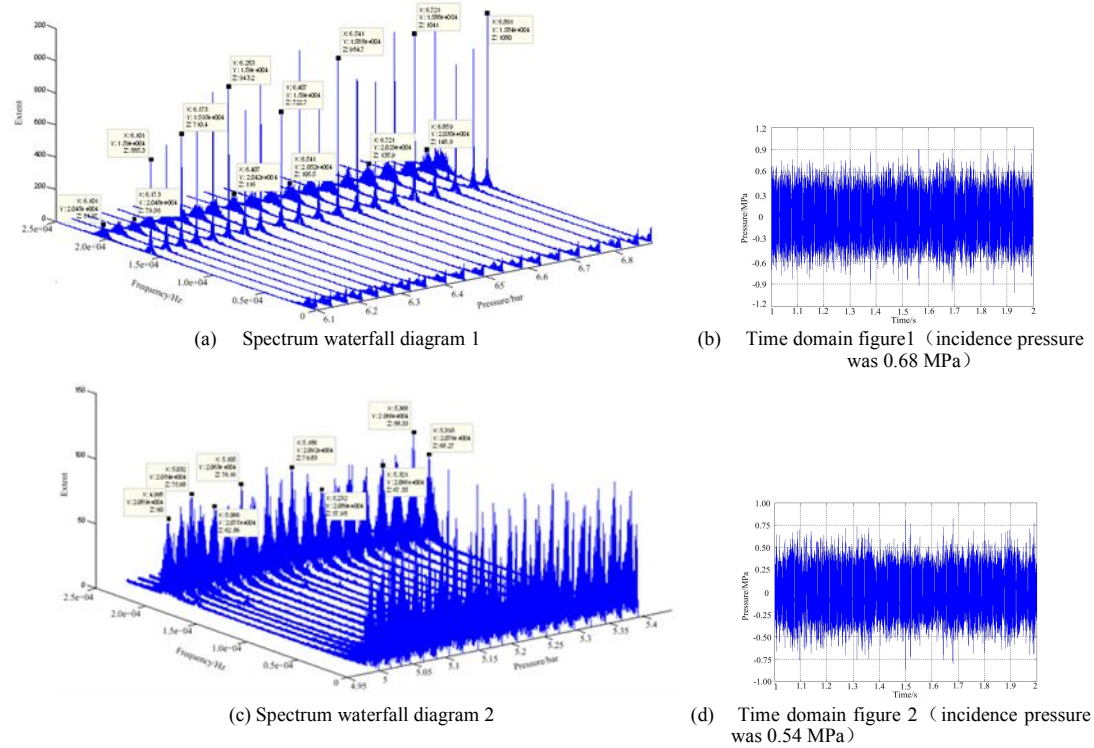


Fig.10 Spectrum waterfall diagram and time domain figure of dynamic pressure of hemispherical resonator bottom (  $D=70\text{mm}$  hemisphere resonator,  $k=70\text{mm}$ ,  $d=4.2\text{mm}$ )

The resonant frequency comparison of various configuration parameters of resonator were drawn, as can be seen from Figure 11 to figure 21. The conclusions are as follows.

(1) Resonators with various sizes have various resonant characteristics under the same curvature. The value and the quantity of resonant frequency are different. The comparison result is: as the size of partial-spherical resonator increases,  $\alpha$ -frequency decreases and the quantity of  $\beta$ -frequency decreases. The resonator size should be neither too large and nor too small. The shock wave focus effectiveness of  $D=74\text{mm}$  partial-spherical resonator is the best.

(2) With the increase of resonator curvature,  $\alpha$ -frequency increase. As the curvature of resonator increase, the dynamic pressure amplitude of resonator bottom decreases when the toroidal incidence nozzle width is the same.

(3) As the incidence angle of resonator increases, the resonant frequency increases. The dynamic pressure amplitude of resonator bottom with  $11^\circ$  incidence angle is more than that of resonator with  $15^\circ$  incidence angle.

(4) As the airflow exit area decreases, the resonant frequency of resonator increases and the dynamic pressure amplitude of resonator bottom increases.

(5) As nozzle diverging angle increases, the highest  $\alpha$ -frequency increases and the quantity of  $\beta$ -frequency increases. Considering the dynamic pressure amplitude of resonator bottom, nozzle diverging angle should be neither too large nor too small; when the nozzle diverging angle is  $30^\circ$ , the dynamic pressure amplitude of resonator bottom is maximal.

(6) As  $L$  increases, the resonant frequency decreases and the dynamic pressure amplitude of resonator bottom decreases.

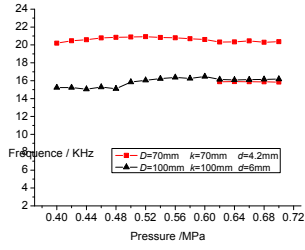


Fig.11 Resonant frequency comparison of various-size hemispherical resonators

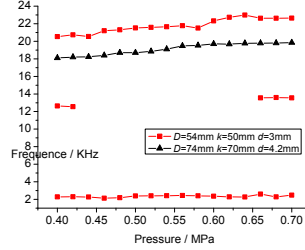


Fig. 12 Resonant frequency comparison of various-size partial-spherical resonators.

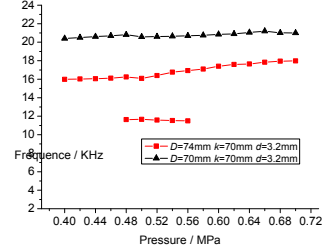


Fig.13 Resonant frequency comparison chart of various curvature resonators (d=3.2mm)

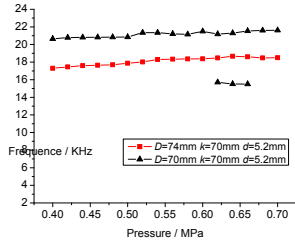


Fig. 14 Resonant frequency comparison chart of various curvature resonators (d=5.2mm)

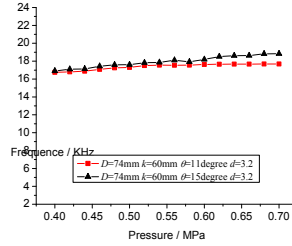


Fig. 15 Resonant frequency comparison chart of resonator with various incidence angles (d=3.2mm)

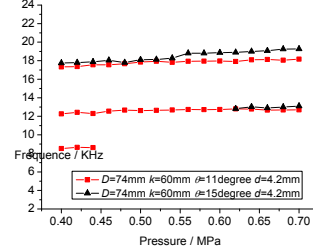


Fig.16 Resonant frequency comparison chart of resonator with various incidence angles (d=4.2mm)

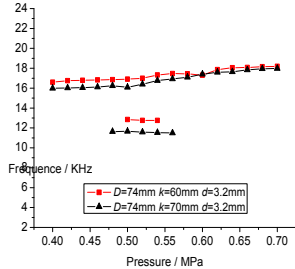


Fig.17 Resonant frequency comparison chart of resonator with various airflow exit areas (d=3.2mm)

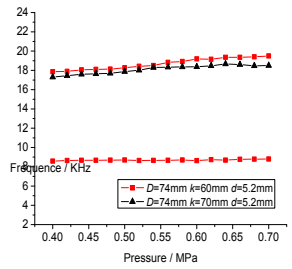


Fig.18 Resonant frequency comparison chart of resonator with various airflow exit area (d=5.2mm)

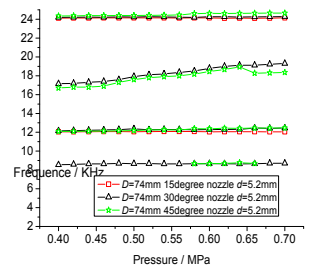


Fig.19 Resonant frequency comparison chart of resonator with various diverging angle nozzles

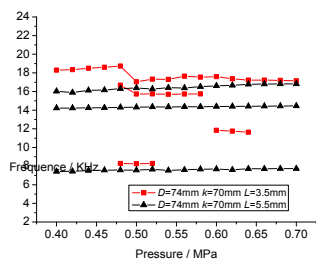


Fig.20 Resonant frequency comparison chart of resonator with various L (incidence angle was 0°)

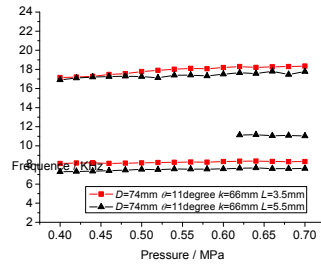


Fig.21 Resonant frequency comparison chart of resonators with various L (incidence angle is 11°)

## 2. Initiation experiments

As can be seen from above research, D=74mm partial-spherical resonator(with d=4.2mm,θ=11°) show best shock wave focusing performance. So D=74mm partial-spherical resonator was chosen to carry out initiation experiments and petrol was used as fuel.

There are three distinct combustion models of operation of the 2-stage rig. For many cases, there is a turbulent flame visible downstream of the resonator cavity. Figure 1 shows a typical image obtained with a color digital video camera. This image reveals that chemical reactions are not complete and therefore there is some loss in performance. The flame jet frequency is 12Hz. In addition, the average amplitude of pressure fluctuations at the resonator bottom are 0.9Mpa. Mach diamonds are visible downstream of the resonator exit (as seem in Figure 22).



Fig.22 Flame jet propagating from aft end of 2-stage rig (Model 1)



Fig.23 Image of the flame structure of second model of combustion (Model 2)

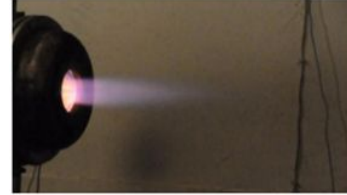


Fig.24 Flame imaging downstream of the resonator cavity during 1.1kHz resonant model of operation (Model 3)

A second model of combustion appears as a long blue flame and the frequency is 4Hz. The amplitude of pressure fluctuations at the resonator bottom are low indicating a lack of unsteady pressure waves that are normally associated with detonations. Overall, this model of combustion is not consistent with detonations. Images of this model of combustion are shown on Figure 23. A third model of combustion appears as a compact, blue flame with a strong 1.1kHz tone. But the amplitude of pressure fluctuations at the resonator bottom are very low. This model of combustion appears when the flame in the pre-combustor blows out. Images of this model of combustion are shown on Figure 24.

We will further investigate the first combustion model to judge whether a detonation is initiated. So further analysis are needed, (1) analysis the pressure time –histories and images ;(2) measure the thrust.

### Acknowledgments

This work was supported by National Natural Science Foundation of China (51406234, 51436008).

### References

- [1]K. Kailasanath, AIAA Journal, Vol. 38, No. 9, pp. 1698-1708, 2000.
- [2]C.M. Brophy and D.W.Netzer, “Effects of Ignition Characteristics and Geometry on the performance of a JP-10/O<sub>2</sub> Fueled Pulse Detonation Engine”, AIAA-99-2635, 35th AIAA Joint Propulsion Conference, Los Angeles, CA, 1999.
- [3]Roy, G.D., Frolov, S.M., Borisov, A.A “Pulsed detonation propulsion: challenges, current status, and future perspective”, Progress in Energy and Combustion Science, 30(2004) 545-672.
- [4]Levin, V.A., Nechaev, J.N., and Tarasov, A.I., “A New Approach to Organizing Operation Cycles in Pulse Detonation Engines”, pp. 223-238 in High-Speed Deflagration and Detonation: Fundamentals and Control, (Ed. G.D. Roy, S.M. Frolov, D.W. Netzer and A.A. Borisov), Moscow 2001.
- [5]Leyva, I.A., Tangirala, V., Dean, A.J., “Investigation of Unsteady Flow Field in a 2-Stage PDE Resonator”, AIAA-2003-0715, 41st Aerospace Sciences Meeting, Reno, NV, 2003.
- [6]Keith R M. Manus, Anthony J. Dean. “Experimental evaluation of a two-stage pulse detonation combustor.” 41st AIAA/ASME/SAE/ASEE joint propulsion conference & exhibit , 2003,AIAA 2003-3773.
- [7]Hao ZENG, Li-ming HE, “Investigation on the influence of jets pressure on detonation initiation via imploding annular shock waves,” Journal of Aerospace Power, Vol.25. No 9,2010.
- [8]Hao ZENG, Li-ming HE, Xiong-wei ZHANG, “Investigation on the influence of jets spout location on detonation initiation via imploding annular shock waves” Journal of propulsion technology, Vol.32. No 3,2011.
- [9]Hao ZENG, Li-ming HE, Xiong-wei ZHANG, “Investigation on the influence of jet width on detonation initiation via imploding annular shock waves” Acta aerodynamica sinica, Vol.29. No 4,2011.